

Low Altitude Wind Simulation Over Mount Saint Helens Using NASA SRTM Digital Terrain Model

M.J. Garcia

Mechanical Engineering
EAFIT University
Medellin, Colombia

P. Boulanger

Computing Science
University of Alberta
Edmonton, Alberta, Canada T6J 2E8

Abstract

On February 11, 2000, the Shuttle Radar Topography Mission (SRTM) was launched into space as part of one of the payload of the Shuttle Endeavor. Using a new radar sweeping technique most of the Earth's surfaces was digitized in 3D in approximately 10 days. SRTM acquired enough data during its mission to obtain a near-global high-resolution database of the Earth's topography. This paper describe how this revolutionary data set can be used to simulate anywhere around the Earth low altitude wind conditions for various atmospheric conditions. More specifically, we will describe the various processing steps necessary to convert this high-resolution terrain model provided by the SRTM database into a Computational Fluid Dynamic (CFD) volumetric mesh that is compatible with an open source CFD solver called OpenFOAM running in parallel on large West-Grid supercomputers. This work is the result of a new virtual wind-tunnel under development at the University of Alberta. In the paper, we present wind flow over the Mount-Saint Helens in the United States for a simple wind flow boundary condition.

1. Introduction

Standards and codes of practice for low altitude wind simulations typically assume terrain to be of homogeneous roughness. In order to deal with real terrain roughness many authors [3] use explicit corrections for specific topographies such as hills or escarpments. For more complex situations many researchers use boundary layer wind tunnel testing to get wind speed and flow distributions. With the fast evolution of computers and algorithms, as well as the availability of high resolution digital terrain models (DTM) across the world, numerical wind simulation or Computational Fluid Dynamics (CFD) Models has become very attractive as they provide a low cost alternative to evaluate wind effects in low altitudes.

Standard computational modelling of the wind is made

through the solution of the Navier-Stokes equation,

$$\frac{\partial \rho \vec{u}}{\partial t} + \nabla \cdot (\rho \vec{u} \vec{u}) - \nabla \cdot \mu \nabla \vec{u} = -\nabla p + \rho \vec{g}, \quad (1)$$

where \vec{u} is the velocity vector, ρ the density, μ the viscosity and \vec{g} the gravitational acceleration vector. Solution is typically implemented using the Reynolds Average Navier Stokes (RANS) or in some cases where better accuracy is needed Large Eddy Simulation (LES) is used. Turbulence flow can be solved using the $k - \epsilon$ model which is only suitable for the case of homogeneous isotropic turbulence. Discretization of the continuous equations is made by the Finite Volume Element Method which results in a set of algebraic equations [7].

In the past, the main problem for solving the Navier-Stokes equation for low altitude wind simulation was the availability of good DTM of a regions or even a whole country. At the macro-scale, some of those DTM were produced by solving stereo correspondence between two or more satellite images of a region produced by high resolution satellites such as SPOT [15] or IKONOS [14]. High resolution DTM of some regions were produced using those images. The problem with satellite imagery is the presence of cloud cover where no DTM data can be recovered. Some techniques such as multi-pass integration could complement DTM in a region but are usually plagued with registration problems that reduce the precision of the model [9]. More recently some excellent [5] DTM were produce using the Canadian RADARSAT images as Synthetic Aperture Radar (SAR) solves the occlusion problem created by the cloud cover. However, stereo correspondence between RADARSAT images is made complicated by diffraction problems of the radar waves, especially near mountain peaks as illustrated in [5]. Others use arial photography to get high resolution coverage of a region. In many of those systems, airplane equipped with precise stabilizer and inertial/GPS systems are used to create a set of stereo pairs that can then be processed to extract very accurate DTM models. In addition to passive stereo to recover DTM other

systems use laser radars (LiDAR) to recover high resolution DTM for small regions. Application of LiDAR were use to recover DTM of forest regions as well as cities [13]. The problem with LiDAR is that it can only recover micro-scale regions as the airplane or helicopter can only fly at low altitude in order to avoid cloud cover and to get enough signal from the probing laser. Attempt to digitize larger regions using a combination of GPS/inertial and data to data registration was performed for regions as large as the whole country of Netherland [18]. What is really needed for low altitude wind simulation is a medium resolution (30 to 100 meters precision) DTM that would cover very large regions or even an entire country.

On February 11, 2000, the Shuttle Radar Topography Mission (SRTM) was launched into space as part of one of the payload of the Shuttle Endeavor. Using a new radar sweeping technique most of the Earth's surfaces was digitized in 3D in approximately 10 days. SRTM acquired enough data during its mission to obtain a near-global high-resolution database of the Earth's topography.

This paper describe how this revolutionary data set can be used to simulate anywhere around the Earth low altitude winds for various atmospheric conditions. More specifically, we will describe the various processing steps necessary to convert this high-resolution terrain model provided by the SRTM database into a CFD volumetric mesh that is compatible with an open source CFD solver called OpenFOAM (Open source Field Operation and Manipulation) running in parallel on large WestGrid¹ supercomputers.

Applications of this combination of high resolution DTM with CFD includes wind energy farm development, flow over buildings, and dispersion of pollution. Wind simulation and prediction near ground and developing of high accuracy maps of this winds to help wind farm developers locate optimum areas of high wind energy potential. Wind farms are the fastest growing energy sector in the world today. Pinard et al [20] uses WEST (Wind Energy Simulation Toolkit) to simulate the wind climate of the southern Yukon Territory's mountainous terrain. WEST uses the mesoscale model MC2 (Mesoscale Compressible Community, [2]) and the linearized microscale model MS-Micro/3R [23] to produce a wind map of a large region. The toolkit has been successfully used to simulate the wind energy potential for several regions across Canada and some other regions. However, Pinard's studies over the Yukon region gave errors of about 40% in wind magnitude and direction. A possible cause of the problem is attributed to the rather greatly modified mesoscale terrain used as surface input to MC2. Finally, a review of wind simulations over complex terrain is found in [3]. It presents a comparative analysis among computational simulations and experiment data showing variations of wind flow over hills, valleys and other terrain con-

figurations.

Another application includes simulation of flows over buildings, civil structures and vehicles. Flows over bluff bodies usually produce strong vortices in their wakes. These vortices produce fluctuating forces on the structure both in stream wise and span wise directions whose prediction is very important [7]. Also pedestrian level winds became important at areas with high population of buildings and in some cases a wind tunnel testing is required in order to approve the construction of new buildings.

A third application of the high interest is the dispersion of pollutants expelled by factories into the atmosphere. It helps predict how contaminants disperse and reach populated areas. Simulation provides a way to relocate factories near cities to minimize pollution effects [17, 4, 1, 12].

2 Format of SRTM Digital Terrain Models

DTM is a representation of elevation data of the earth surface. They are organized in several files which contains latitude, longitude and elevation coordinates of points over the earth surface. One of the most complete collection of high resolution DTM was acquire by the Shuttle Radar Topography Mission (SRTM)[19, 6]. One can see in Figure 1 an illustration of the radar measuring system and in Figure 2 an illustration of the earth coverage performed during the 10 days. Topographic data was collected for dry lands (excluding water masses) between 56 degree latitude South and 60 degree latitude North, covering about 80% of the total surface.

The gathered data was processed and organized in segments covering one degree latitude by one degree longitude. Every segment was saved in a distinct file. Every file is organized as a grid of n rows and m columns of samples whose distance is either one arc second (1/3600 of degree) for United States (SRMT) and three arc seconds (SRMT3) for the rest of the world. In the case of SRTM3 the number of rows and columns is $n = m = 1201$. The rows on North and South border, as well as columns on East and West border, will be identical (and consequently will overlap) to rows/columns of adjacent file borders (see Figure 3).

One arc second measured at equator, corresponds approximately to 30 meters, so two sampling points in a STRM3 file are distant roughly 90 meters from each other. This approximation will deteriorate as one move away from the equator in the direction of the poles.

By convention SRTM files names, with .HGT extension, recall the latitude and the longitude of the geometrical sample located in the lower left corner of the segment contained within the file. For example, Figure 3 shows the structure

¹Western Canada Research Grid



Figure 1: Illustration of the NASA SRTM radar measurement system. (Image from NASA Website)

of a file with name N20W100.HGT. It will contain the samples from longitude 20 degree North to 21 degree North and from latitude 100 West to 99 West.

Every sample is represented with a 16 bit signed integer, row ordered. Integer coding is *big endian*, meaning that the first byte read is the most significant and the second is the less significant. The number associated with each sample corresponds to its elevation measured in meters with respect to the WGS84 EGM96 geoid (the geoid is a rotational solid used in geodesy, that approximates the shape of the earth better than a sphere or an ellipsoid). The data files are not perfect and some *voids* can be present. They are due to shadows or water reflection creating distortions. Data sam-

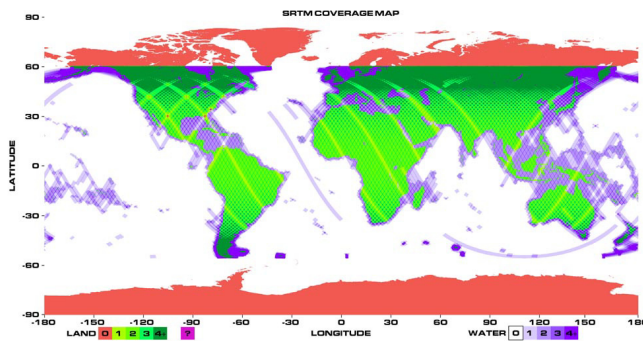


Figure 2: Illustration of the NASA SRTM measured earth coverage. (Image from NASA Website)

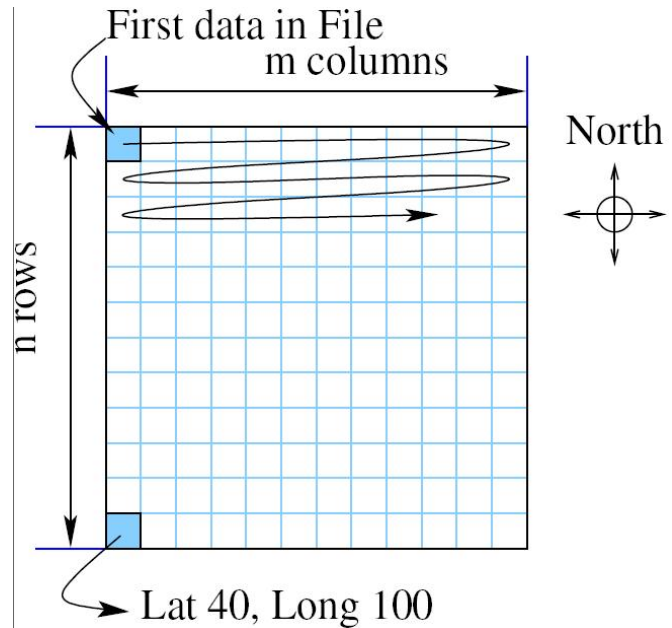


Figure 3: Description of a .HGT file structure. The name file in this case is N20W100.HGT

ples corresponding to these voids are given a conventional code value of -32768.

Processed data can also be retrieved through the Seamless Data Distribution System (SDDS) of the U.S. Geological Survey (USGS) and the EROS Data Center (EDC) [22]. The main feature is that the user can define an area of interest by drawing a box, defining coordinates, or use available templates to cut out the area. They also offer a variety of DTM formats.

3 Definition of the CFD Domain for Wind Study

A CFD domain is created from the DTM information and it should covers a large enough portion to guaranty accuracy in the simulation. For low altitude wind simulation a volume of air over the surface constitutes the CFD domain.

3.1 Filling Shadow Regions

Data from the SRMT should be completed to generate the domain. Voids can be filled in different ways using several interpolation techniques. Also, information from other sources, like other DTM databases or GPS measurements, can be used to complete the data.

A simple interpolation technique using information from the closest points around a void \vec{x} is used to interpolated the

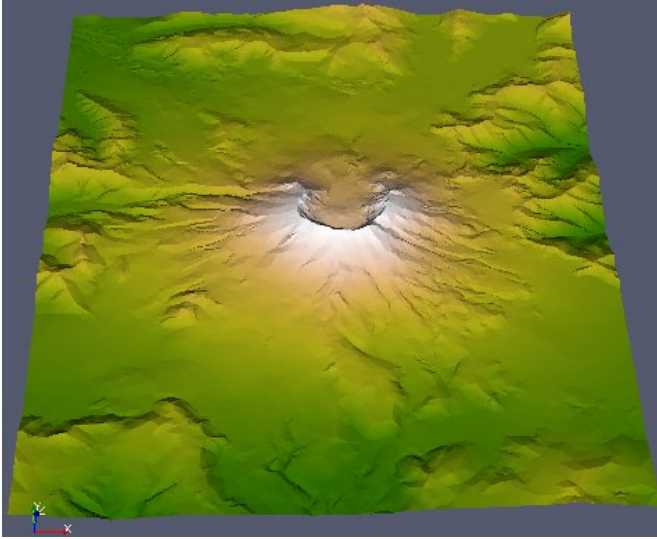


Figure 4: Digital terrain model of mount Saint Helens region produced by SRTM.

points inside the void. The interpolation function used is defined by:

$$z(\vec{x}) = \frac{1}{n} \sum_{\vec{q}_j \in \Omega_x} w_j z(\vec{q}_j), \quad \Omega_x = \left\{ \vec{q}_j \mid \|\vec{x} - \vec{q}_j\| < r \right\}, \quad (2)$$

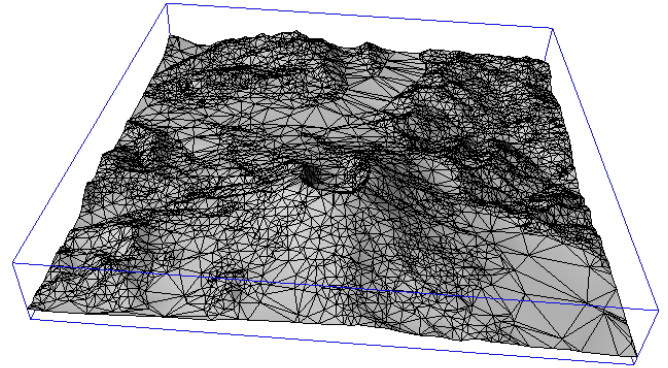
with w_j a weight factor and $r \in \mathbb{R}$. This weighted average can be further enhanced if a least square approximation is taken over a patch $\|\vec{x} - \vec{q}_j\| < r$ around the void [8].

During this project, a new hole filling algorithm was developed using Radial Basis Functions. We are currently testing its capability for DTM applications. One can refer to the paper by Branch et al. [11] for more details.

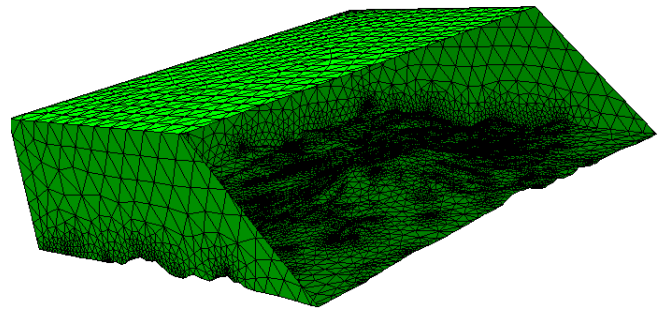
3.2 From Surface Mesh to Volumetric Mesh for CFD

The finished DTM data is transformed into a regular grid of triangular elements, e.g. a 2-manifold with border that represents the terrain surface. The SRMT data files cover an approximate area of 108×108 km. As SRMT3 data is sampled at every 3 arc sec it will contain in total 1'442,401 equidistant points. This surface can be efficiently decimated preserving the curvature detail by suppressing points at low curvature regions. Depending on the topography of the terrain it can be reduced up to 15 to 10 % of the original data while keeping the approximation error low. In order to do so we used POLYWORKS IMCompress to perform this decimation. The algorithm eliminates sequentially the triangle that produce the smallest error until an approximation threshold is reached.

CFD domain consist of a volume of air over the terrain surface. It can be generated by projecting vertical walls along the sampled terrain boundary and then intersecting the resulting shell with a horizontal plane at a given height h . The final manifold must be closed and topologically correct (See Figure 5b).



(a) Digital terrain model after decimation using POLYWORKS IMCompress.



(b) The CFD domain created over the decimated digital terrain model.

Figure 5: Decimated mesh and volumetric domain for CFD analysis.

Once a correct superficial mesh of the domain is obtained a volumetric mesh needs to be generated. An ideal mesh for the volume element method consist of hexahedral elements. However, it is very complex to obtain automatically and there are several research groups working in this field. An alternative to structured hexahedral meshes are the so called unstructured tetrahedral meshes. They should be used with caution when using volume element method and orthogonal correctors should be used to insure convergence of the CFD solver. In this study, tetrahedral meshes are generated using Netgen [21]. Netgen Algorithm can be summarized as follows. It starts from a superficial mesh that does not require to be of a good quality but must be topologically correct. Netgen starts by computing the corner points and edges. These are meshed into segments and the faces are meshed by an advancing front surface mesh generator. Faces meshes are optimized to obtain a good

quality superficial mesh. Individual sub-domains are filled with tetrahedral using a fast Delaunay triangulation algorithm. This generates most of the elements but often fails to complete the whole domain. Then, a slower back-tracking rule-based algorithm takes over and completes the task. As a final step, the volumetric mesh is optimized by a series of node-movements, element swapping's and splitting's [21].

Mesh grading towards the terrain is not necessary when using the standard $k - \epsilon$ model with wall functions since the flow in the near wall cell is modelled, rather than having to be resolved. Nevertheless, due to the size of the domain a moderate grading is maintained in order to reduce the mesh size.

4 Definition of Boundary Conditions

Due to the boxed shape of the domain, boundary surfaces are the terrain surface, the south, north, east and west walls, and the top surface.

Wind velocity at input boundary can be obtained using a simple logarithmic rule that makes use of the surface roughness z_0 for each site, namely

$$u(z_p) = u(z_m) \frac{\ln \frac{z_p}{z_0}}{\ln \frac{z_m}{z_0}}, \quad (3)$$

where the wind speed $u(z_m)$ measurement (or modelled) at height z_m is projected vertically to new speed $u(z_p)$ and height z_p . This logarithmic projection is done instead of obtaining the wind speeds directly from the model for the exact heights at which the measurements were made. This approach requires wind measurements to extrapolate the wind profile at the entrance wall.

Fictitious wind scenarios can be created to help understand typical real conditions over a geographic area. In such case several sets of boundary conditions should be analyzed. Wind profiles over input boundaries can be obtained by applying

$$u(z_p) = a e^{-\left(\frac{z-c}{b}\right)^2} + m, \quad (4)$$

with a (amplitude), b (wide), c (centre) and m (offset), factors that control the shape of the profile function. Combination of these functions allows to create velocity profiles similar to the one found in nature. Other boundary conditions include:

- Uniform input $\vec{u} = (10, 0, 0)$ m/s;
- Outlet (with fixed pressure $p = 0$ Pa;
- No-slip walls over the terrain;
- Wall functions over the terrain;

- symmetry condition over the top wall $\nabla \vec{u} \cdot \hat{n} = 0$.

It should be noticed that, as well as in a wind tunnel, accurate results are only expected at some distance from the boundary walls.

5 Physical Model

From all the methods, Direct Numerical Simulation (DNS) produces the most accurate results. It is however, the most expensive of all the solving methods as it maintains small variations of the turbulent flow. Large scale motion is much more energetic than small scale motion. It is responsible for transport of the conservative properties. It has complete information of the flow. Large Eddy Simulation (LES) works with large scale motion while neglecting low scale motion. It is a three dimensional time dependent approach which is computationally expensive but less costly than DNS. As it only model large scale motion it is also less accurate than DNS [16]. The objective of flow simulation is to predict selected properties of the flow at minimum cost. It is not easy to predict how well each method will work. In many situations RANS methods are successful [3] for modelling of low altitude wind flow over complex terrain.

In this implementation, the low altitude wind over the terrain is simulated using the OpenFoam toolkit. OpenFOAM is the Open Source Field Operation and Manipulation (OpenFOAM) C++ libraries used primarily to create applications. The applications fall into two categories: solvers, that are each designed to solve a specific problem in continuum mechanics; and utilities, that are designed to perform tasks that involve data manipulation. The OpenFOAM distribution contains numerous solvers that includes from basic flows as Laplacian, potential, steady state and transient incompressible flow, non-newtonian flow, compressible flow, transonic, supersonic, multiphase flow, direct numerical simulation (DNS) and large eddy simulation (LES), heat transfer and buoyant flow, among others [24, 10].

For low altitude wind simulation the governing equations are: the mass continuity:

$$\frac{\partial \rho}{\partial t} + \nabla \cdot (\rho \vec{u}) = 0. \quad (5)$$

and the momentum conservation equation:

$$\frac{\partial \rho \vec{u}}{\partial t} + \nabla \cdot (\rho \vec{u} \vec{u}) + \nabla \cdot (\mu \nabla \vec{u}) = -\nabla p + \rho \vec{g}. \quad (6)$$

In the $k - \epsilon$ model two extra equations are needed: one for

closure and one for the transport equations for k and ε :

$$\frac{\partial(\rho k)}{\partial t} + \nabla \cdot (\rho \vec{u}k) = \nabla \cdot \left(\left(\mu + \frac{\mu_t}{\sigma_k} \right) \nabla k \right) + P_k - \rho \varepsilon, \quad (7)$$

$$\frac{\partial(\rho \varepsilon)}{\partial t} + \nabla \cdot (\rho \vec{u}\varepsilon) = \nabla \cdot \left(\left(\mu + \frac{\mu_t}{\sigma_\varepsilon} \right) \nabla \varepsilon \right) + \quad (8)$$

$$\frac{\varepsilon}{k} (C_{\varepsilon 1} P_k - C_{\varepsilon 2} \rho \varepsilon) \quad (9)$$

where μ_t is the coefficient for turbulent viscosity and is linked to the turbulent kinetic energy k and dissipation ε by $\mu_t = \rho C_\mu \frac{k^2}{\varepsilon}$. The various constants of the turbulence model [7] are empirically determined and taken for the $k-\varepsilon$ model as: $C_\mu = 0.09$, $C_1 = 1.44$, $C_2 = 1.92$, $\sigma_k = 1$, and $\sigma_\varepsilon = 0.76923$.

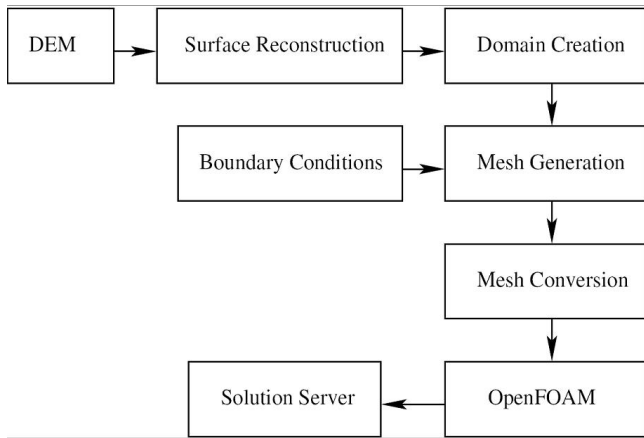


Figure 6: Block diagram of the wind flow simulation process.

To guaranty convergence of the solution an initial field is needed. It can be obtained by solving for potential flow φ over the domain by

$$\nabla^2 \varphi = 0 \quad (10)$$

and solving for \vec{u} from

$$\text{grad } \varphi = \vec{u}. \quad (11)$$

A block diagram of the simulation process is illustrated in Figure 6. Topology of the terrain is obtained from a DTM as a SRTM or BIL file. The surface is reconstructed and the voids filled producing an optimum 2-manifold with border representing the surface of the terrain. A volume is completed by intersecting a cuboid with this surface so that the result is a box with the lower side replaced by the terrain surface. Boundary conditions are set to the domain and a tetrahedral mesh is generated. This mesh is in turn converted into a OpenFOam format. The partial differential

equations are solved and the solution is visualized using ParaFoam an open source viewer specialized for CFD applications.

5.1 Low Altitude Wind Flow Over Mount Saint Helens

This example simulates the low altitude wind over Mount Saint Helens in the United States. The coordinates are $46^\circ 11' 28''$ N and $122^\circ 11' 39''$ W. A view of the terrain after the surface mesh is generate is shown in Figure 4. The CFD domain is generates with a box size of 18838 m in the x (West-East) direction, 17476 m in the y (South-North) direction, and the top face is located at a height of 6000 m. For this section, the minimum height of the terrain is 468 m and the maximum height 2490 m. The problem was solved using a mesh of 262,078 elements. The kinematic viscosity of air was taken as $\nu = \mu/\rho = 18.1 \times 10^{-6}/1.293 = 14.0 \mu \text{ m}^2/\text{s}$. The flow was calculated with standard $k\varepsilon$ model as described in the previous section. Figure 7 shows stream lines near the mountain summit.

6 Conclusion

As mentioned previously, wind simulation is being increasingly used over the past decades to analyze the effects of low altitude winds on structures such as: building, wind mills, people, and much more. Recent development in High Performance Computers (HPC) has made possible the simulation of more accurate models in a reasonable time frame. This article presents a methodology for wind analysis that solve many issues associated to low altitude wind simulation. The results compares qualitatively to the one found in the literature but further research needs to be done in order to validate the results. The simulation presented here use a Reynolds average model with turbulence thought the $k-\varepsilon$ model using the OpenFOAM toolkit. No compressibility effects where taken into account and therefore buoyancy effects are depreciated.

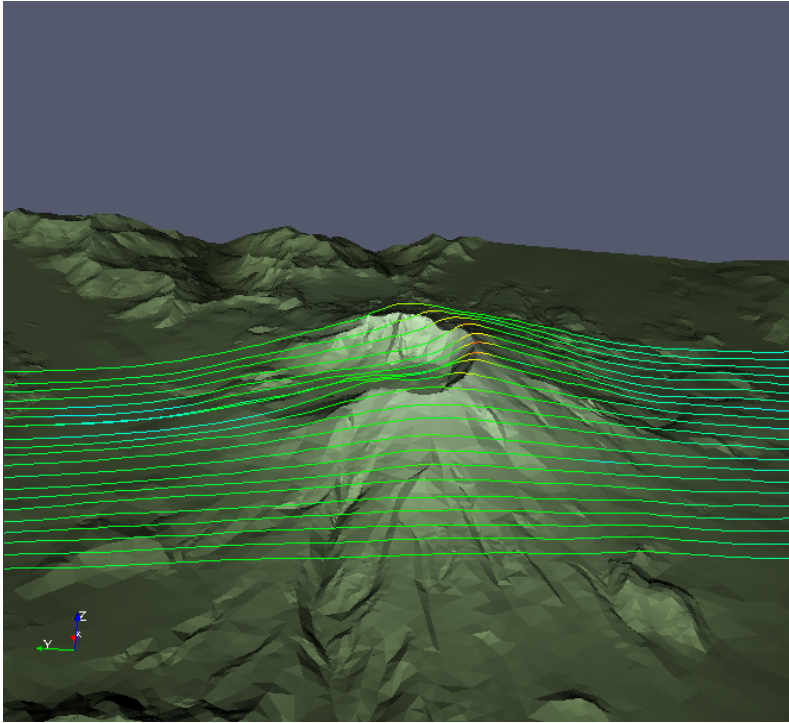
Future research include the study of mesh resolution, parallel performance, large eddy simulations and boundary conditions that adjust to real situations. We are also studying new algorithm to automatically fill holes using a curvature analysis and a radial basis function interpolator.

Acknowledgments

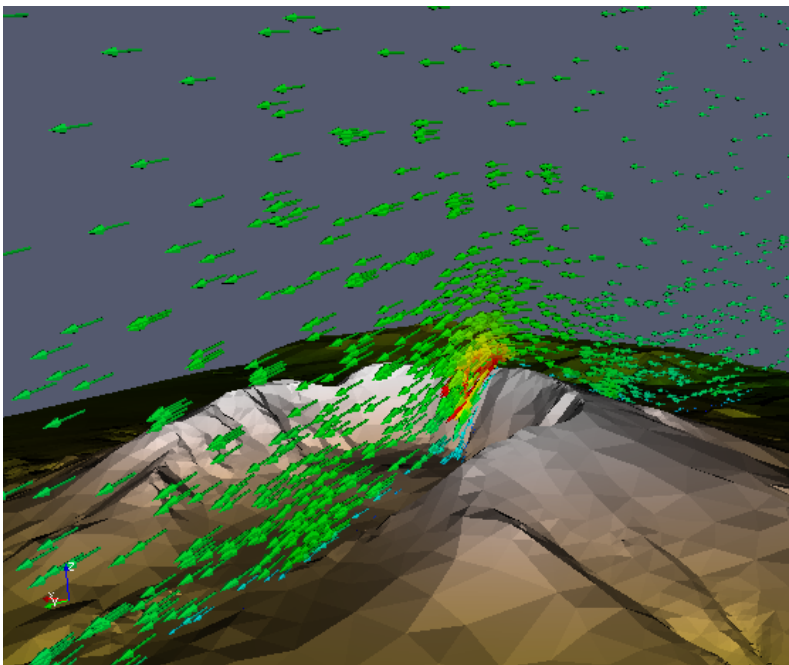
This work was partially funded by Alberta's Informatics Center of Research Excellence (iCORE) as well as by NSERC.

References

- [1] Walton A, Cheng A.Y.S., and Yeung W.C. Large-eddy simulation of pollution dispersion in an urban street canyon-part i: comparison with field data. *Atmospheric Environment*, 36(22):3601–3613, 2002.
- [2] R. Benoit, M. Desgagne, P. Pellerin, S. Pellerin, Y. Chartier, and S. Desjardins. The canadian mc2: A semi-lagrangian, semi-implicit wideband atmospheric model suited for finescale process studies and simulation. *Mon. Wea. Rev.*, 125:23822415, 1997.
- [3] G. T Bitsuamlak, T. Stathopoulos, F. ASCE, and C B. Numerical evaluation of wind flow over complex terrain: Review. *Journal of Aerospace Engineering*, 17(4):135–144, Octobre October 2004.
- [4] Paul Dawson, David E. Stock, and Brian Lamb. The numerical simulation of airflow and dispersion in three-dimensional atmospheric recirculation zones. *Journal of Applied Meteorology*, 30(7):1005–1024, 1991.
- [5] Y. Kurucu F. Balyka, A. Alkyba and Z. Alkyb. Validation of radargrammetric dem generation from radarsat images in high relief areas in edremit region of turkey. *The International Archives of the Photogrammetry, Remote Sensing and Spatial Information Sciences*, 34, 2004.
- [6] T.G. Farr and M. Kobrick. Shuttle radar topography mission produces a wealth of data. *Amer. Geophys. Union Eos*, 81:583–585, 2000.
- [7] J. H. Ferziger and M. Perić. *Computational Methods for Fluid Dynamics*. Springer, 3rd edition, 2002.
- [8] Manuel J. García. *Fixed Grid Finite Element Analysis in Structural Design and Optimization*. PhD. Thesis The University of Sydney, Sydney, 1999.
- [9] Yi-Ping Hung, Chu-Song Chen, Kuan-Chung Hung, Yong-Sheng Chen, and Chiou-Shann Fuh. Multipass hierarchical stereo matching for generation of digital terrain models from aerial images. *Machine Vision and Applications*, 10(5/6):280–291, 1998.
- [10] H. Jasak, H.G. Weller, and N. Nordin. In-cylinder CFD simulation using a C++ object-oriented toolkit. SAE Technical Paper 2004-01-0110, 2004.
- [11] F. Prieto J.W. Branch and P. Boulanger. Automatic hole-filling of triangular meshes using local radial basis function. *Submitted to 3DPVT 2006*, 2006.
- [12] Si-Wan Kim, Chin-Hoh Moeng, Jeffrey C. Weil, and Mary C. Barth. Lagrangian particle dispersion modeling of the fumigation process using large-eddy simulation. *Journal of atmospheric Sciences*, 62(6):1932–1946, 2005.
- [13] K. Kraus and N. Pfeifer. Advanced dtm generation from lidar data. *International Archives of Photogrammetry and Remote Sensing*, 34(3/W4):23–30, 2001.
- [14] C.Y. Lo L.C. Chen and J.Y. Rau. Generation of digital orthophotos from ikonos satellite images. *Journal of Survey Engineering*, pages 73–78, 2003.
- [15] H. Lee L.C. Chen and S.C. Lee. Dtm generation using spot digital data. *Archive of ISPRS. Com III*, 129(2):100–109, May May 1988.
- [16] A. Leonard. Energy cascade in large eddy simulations of turbulent fluid flow. *Adv. Geophys.*, 18A:237, 1974.
- [17] Paolo Monti and Giovanni Leuzzi. Development of numerical model for dispersion over complicated terrain in the convective boundary layer. *International Journal of Environment and Pollution*, 25(1-4):239–250, 2005.
- [18] S. Filina M. Sesterb Y. Doytshera N. A. Akela, K. Kre-meikeb. Dense dtm generalization aided by roads extracted from lidar data. *ISPRS WG III/3, III/4, V/3 Workshop on Laser scanning 2005*, September 2005.
- [19] National Geospatial-Intelligence Agency (NGA), the National Aeronautics, and Space Administration (NASA). The shuttle radar topography mission (srtm). <http://www2.jpl.nasa.gov/srtm/>, 2000.
- [20] Jean-Paul Pinard, Robert Benoit, and Wei Yu. A WEST wind climate simulation of the mountainous yukon. *Atmosphere-ocean*, 43(3):259282, 2005.
- [21] Joachim Schberl. *NETGEN*. Johannes Kepler University Linz., Austria, 4.3 edition, 2005. <http://www.hp fem.jku.at/netgen>.
- [22] US. Geological service. Seamless data distribution system. <http://seamless.usgs.gov/>, 2003.
- [23] J. Walmsley, D. Woolridge, and J. Salmon. Ms-micro/3 user's guide, 1990.
- [24] H.G. Weller, G. Tabor, H. Jasak, and C. Fureby. A tensorial approach to computational continuum mechanics using object orientated techniques. *Computers in Physics*, 12(6):620 – 631, 1998.



(a) Flow lines over Mount Saint Helens.



(b) Detail of the flow lines near the summit.

Figure 7: Low altitude velocity wind flow over Mount Saint Helens.